TABLE 1. Patient Characteristics

Characteristic	Value
No. of patients	30
Age (yr)	
Median	64
Range	44–87
Gender	
Male	18
Female	12
Histology	
Adenocarcinoma	25
Squamous-cell carcinoma	3
Large-cell carcinoma	2
Stage	
IIIB	4
IV	26
Metastatic sites	
Pulmonary	16
Bone	12
Brain	11
Others	4
ECOG performance status	
0	20
1	6
2	4
Prior treatment	
Yes	6
Operation	6
Radiation	3
No	24
Smoking	
Yes	20
Pack-years (mean ± SD)	51 ± 39
No	10

ECOG, Eastern Cooperative Oncology Group.

TABLE 2. Response to Gefitinib Monotherapy and Prognostic Factors*

	No.	PR	SD	PD	RR (%)	*p* Value	DCR (%)	*p* Value
Total	30	10	9	11	33.3		63.3	
Prognostic factors								
Gender								
Male	18	4	4	10	22.2	0.14	44.4	0.018
Female	12	6	5	1	50.0		91.7	
Smoking habit								
Smoker	20	5	5	10	25	0.231	50	0.049
Nonsmoker	10	5	4	1	50		90	
Histologic type								
Adenocarcinoma	25	10	8	7	40	0.139	72	0.327
Nonadenocarcinoma	5	0	2	3	0		40	
PS								
0–1	26	8	8	10	30.8	0.584	61.5	0.999
2	4	2	1	1	50		75	
Clinical stage								
IIIb	4	2	1	1	50	0.584	75	0.999
IV	26	8	8	19	31		62	
Prior treatment								
Yes	24	9	5	10	37.5	0.999	58.3	0.215
No	6	1	4	1	16.7		83.3	

*RR and DCR were compared between prognostic factors using Fisher's exact test.
*PR, partial response; SD, stable disease; PD, progressive disease; RR, response rate; DCR, disease control rate.

TTP and OS

At a median follow-up of 12 months, 20 patients had died and 26 patients were refractory or had become resistant to gefitinib monotherapy. Median TTP was 3.3 months (range, 0.3–19.6 months) and median OS was 10 months (range, 1.7–21.4 months) (Figure 1. Duration of response for patients with partial response was 5.8 months. OS and TTP were not affected by histologic type, smoking, PS, stage, or prior treatment. However, there was a significant difference in survival in gender (median survival time, >12 months in female patients versus 7.7 months in male patients; log-rank test, $p < 0.04$; Wilcoxon test, $p < 0.04$).

Tolerability

Table 3 shows drug-related adverse events. Twenty-six patients (86.7%) experienced drug-related adverse events, most of which were mild. Frequent adverse events included diarrhea, skin rash, and elevated transaminases. Twenty-two patients experienced skin toxicities, such as acne, pruritus, and rash. Grade 3 skin toxicities were observed in two patients, but these resolved spontaneously during treatment. Diarrhea was observed in 12 patients (40.0%) and was controlled with antidiarrheal agents such as loperamide. One patient developed grade 3 diarrhea, which required temporal interruption of therapy. Two patients developed drug-related pneumonitis; both were treated with steroid therapy, antibiotics, and oxygen inhalation and recovered within a few weeks. These patients were smokers and had not received thoracic radiotherapy. No patients experienced hematologic toxicities.

Postgefitinib Treatment

Twenty-five patients became resistant or were refractory to gefitinib monotherapy. Eight of these patients received neither chemotherapy nor radiotherapy because of deterioration of PS in four patients and withdrawal of informed consent to chemotherapy in three patients. One patient underwent palliative surgery and two received radiotherapy for symptomatic brain metastases. Fifteen patients received chemotherapy as postgefitinib treatment (platinum-based chemotherapy in 14 patients and vinorelbine monotherapy in one patient). Five patients achieved PR and four showed SD by the second-line chemotherapy.

EGFR Mutations in Tumor Samples

Twenty tumor samples were obtained from 15 patients retrospectively. Sequencing of exons 18, 19, and 21 in *EGFR* was performed in 12 of 20 samples under the same PCR conditions. *EGFR* mutations were detected in four tumor

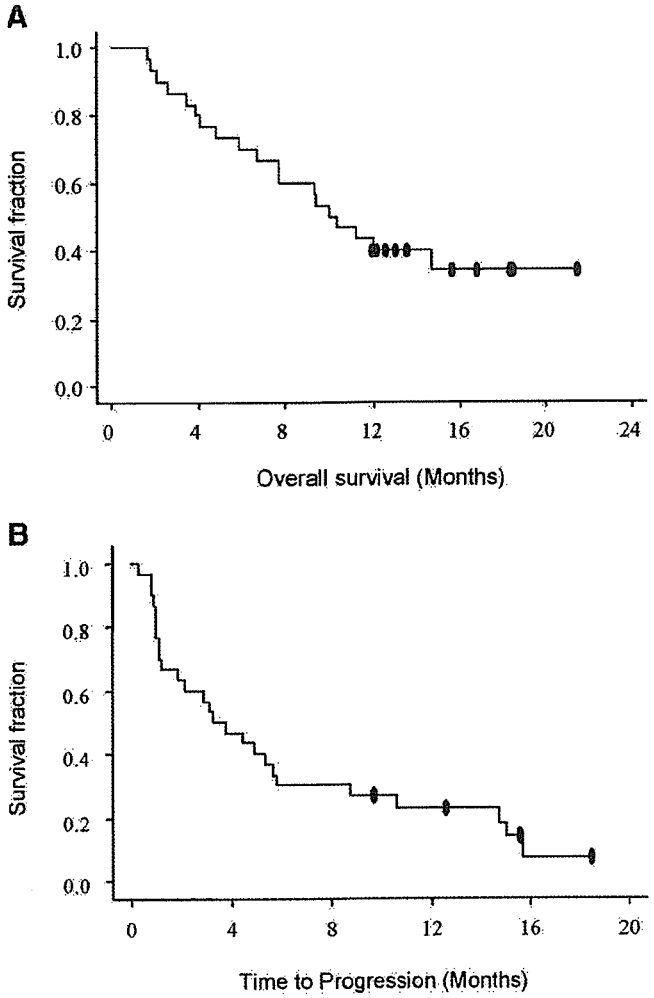

FIGURE 1. Kaplan-Meier curve showing (*A*) overall survival and (*B*) time to progression in all patients.

samples (33.3%). Three of them had a 15–base pair deletion (E746_A750del) in exon 19. Another of them had L858R in exon 21. The histologic types in patients with *EGFR* mutations were adenocarcinoma in three and large-cell carcinoma in one. All patients with E746_A750del in tumor samples had adenocarcinoma. The responses to gefitinib in these four patients were PR in two, SD in one, and PD in one. There were no responders among nine patients without an *EGFR* gene mutation.

EGFR Mutations in Serum Samples

The serum DNA in serum samples from 27 NSCLC patients was examined. Serum DNA was detected in all 54 samples at concentrations of up to 1720 ng/ml.

Exon 19 of *EGFR* in pretreatment serum samples obtained from 21 of 27 patients (77%) was detected (Figure 2 *A*). The lower band was also detected in 10 of 27 (37%) pretreatment serum samples. Sequencing of the PCR products confirmed that the upper and lower bands corresponded to wild-type and E746_A750del, respectively (Figure 2 *B*). No

TABLE 3. Drug-Related Adverse Events

	NCI-CTC Grade	No. of Patients	%
Diarrhea	1	8	26.7
	2	3	10.0
	3	1	3.3
Nausea	1	8	26.7
	2	2	6.7
	3	0	0.0
Vomiting	1	2	6.7
	2	0	0.0
	3	0	0.0
Skin toxicity	1	15	50.0
	2	5	16.7
	3	2	6.7
Elevation of transaminases	1	4	13.3
	2	1	3.3
	3	2	6.7
Pneumonitis	1	0	0.0
	2	0	0.0
	3	2	6.7

NCI-CTC, National Cancer Institute Common Toxicity Criteria.

point mutation in exon 18, 19, or 21 was detected in the PCR products from serum samples. Wild-type *EGFR* was detected in all 10 of the deletion-positive cases. The pattern of bands was reproducible when using another primer set.[13]

When compared according to histologic type, E746_A750del was detected in eight of 25 (32%) cases of adenocarcinoma, in zero of three cases of squamous carcinoma, and in two of two cases of large-cell carcinoma (Table 4). In contrast, the serum *EGFR* status was not correlated statistically with either the clinical response, the gender, or the recorded adverse effects (Table 5).

In serum samples obtained after the initiation of gefitinib treatment, 19 of 27 (70%) cases were wild-type–positive and 14 of 27 (52%) cases were deletion-positive (Figure 2 *C*). In the posttreatment serum samples, E746_A750del was more frequently observed. Furthermore, the deletional mutant of *EGFR* was significantly more frequently observed in samples from patients who showed a PR or SD (12 of 16 cases [75%]) than in samples from patients with PD (two of 11 cases [18%]) ($p = 0.0063$, Fisher's exact test) (Table 6). The deletional mutant *EGFR* was more frequently detected in female patients (six of nine cases [67%]) than in male patients (eight of 18 cases [44%]), but this difference was not significant (Table 6). No correlations were seen statistically between the presence of mutation and the adverse effects.

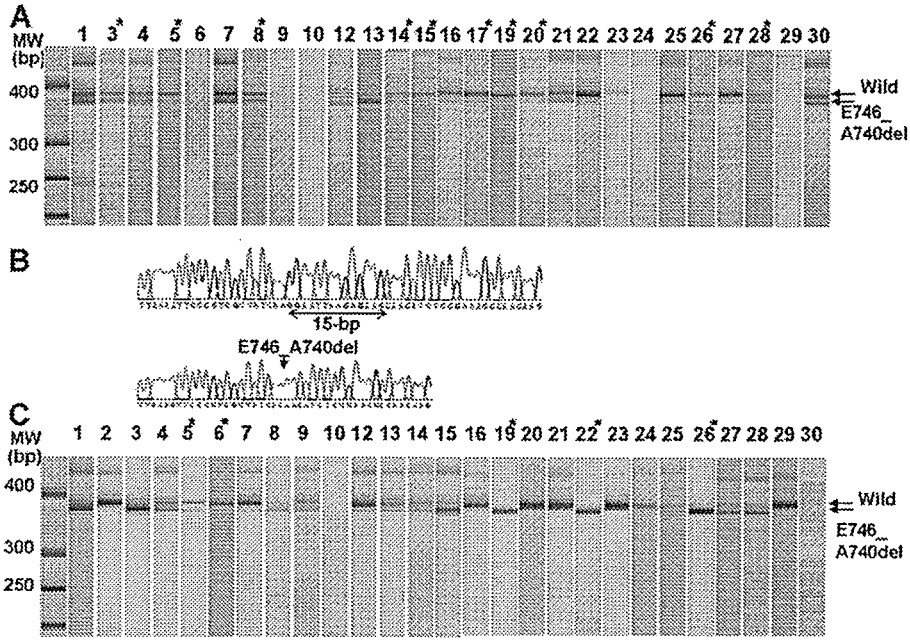

FIGURE 2. (*A*) Detection of genomic *EGFR* in the serum of pretreatment patients. (*B*) The sequences of the PCR products from patient 19 (days 0 and 14) are shown. (*C*) PCR of the serum samples obtained on day 14. Serum-derived genomic DNA PCR was performed. Exon 19 of *EGFR* in serum obtained from the patients was amplified by PCR, and the products were detected using a Bioanalyzer. A second round of PCR (20 cycles) was performed when no band was detected in the first round of PCR (30 cycles). Row numbers indicate the patient number. *Band detected in the first round of PCR.

TABLE 4. Frequency of Serum *EGFR* in Lung Cancer Patients According to Histology and Response to Gefitinib*

	Pre		Post	
	Wild	Deletion	Wild	Deletion
Adenocarcinoma	18/23	8/23	15/22	13/22
Squamous-cell carcinoma	1/2	0/2	3/3	0/3
Large-cell carcinoma	2/2	2/2	1/2	1/2

*A total of 27 samples were obtained from 28 patients both before and after treatment. A pretreatment sample of patient 2 and a posttreatment sample of patient 17 were lacking.

TABLE 5. Frequency of Serum *EGFR* in Lung Cancer Patients According Response to Gefitinib and Gender: Detection of Deletion-Type Mutation on Day 0*

	+	–	*p* Value
Response			
PR/SD	8	9	
PD	2	8	0.2305
Gender			
Male	5	12	
Female	5	5	0.4153

*A total of 27 samples were obtained from 28 patients both before and after treatment. A pretreatment sample of patient 2 and a posttreatment sample of patient 17 were lacking. SD, stable disease; PD, progressive disease; PR, partial response; +, deletion-positive; –, wild-type.

Comparison of *EGFR* Mutation Status between Tumor Samples and Serum Samples

Pairs of tumor samples and serum samples were obtained from 12 patients retrospectively (Table 7). The *EGFR* mutation status in the tumors was consistent with those in serum of seven of 12 of the paired samples. Among the other five patients, *EGFR* mutation was negative in the tumor and positive in the serum in four patients, and in the other patient it was positive in the tumor and negative in the serum, from whose tumor sample L858R was detected.

TABLE 6. Frequency of Serum *EGFR* in Lung Cancer Patients According to Response to Gefitinib and Gender: Detection of Deletion-Type Mutation on Day 14*

	+	–	*p* Value
Response			
PR/SD	12	4	
PD	2	9	0.0063
Gender			
Male	8	10	
Female	6	3	0.4197

*A total of 27 samples were obtained from 28 patients both before and after treatment. A pretreatment sample of patient 2 and a posttreatment sample of patient 17 were lacking. SD, stable disease; PD, progressive disease; PR, partial response; +, deletion-positive; –, wild-type.

DISCUSSION

The overall response of 33.3% in this phase II study was comparable not only to that achieved in Japanese population enrolled in the IDEAL-1 trial (27.5%)[7] but also to a retrospective analysis conducted of patients in Japan.[22] Gefitinib monotherapy appeared to be equally effective in patients with chemotherapy-naive NSCLC and in patients with pretreated NSCLC.

Drug-related adverse events were generally mild compared with cytotoxic chemotherapy. Grade 3 pulmonary toxicities were observed in two patients. In this study, the

TABLE 7. *EGFR* Mutation Status in Tumor Samples and Serum Samples*

					EGFR Mutation Status			
					Serum Samples			
					Pre		Post	
No.	Gender	Histology	Response	Tumor Sample	Wild	Mutation	Wild	Mutation
43	M	Large	SD	Wild	+	+	–	+
45	M	SCC	PD	Wild	ND	ND	+	–
52	F	SCC	PD	Wild	+	–	+	–
53	M	Adeno	PD	Wild	–	–	+	–
55	M	Adeno	PR	L858R	+	+	–	–
57	F	Adeno	SD	Wild	–	–	+	+
61	M	Large	PD	E746-A750 del	+	+	+	–
64	M	Adeno	PD	Wild	+	–	+	–
70	M	Adeno	PD	Wild	+	+	+	–
72	M	Adeno	SD	E746-A750 del	+	–	–	+
75	F	Adeno	PR	E746-A750 del	+	+	+	+
77	M	Adeno	PD	Wild	+	–	+	+

*Pairs of both tumor samples and serum samples were obtained from 12 patients. M, male; F, female; SD, stable disease; PD, progressive disease; PR, partial response; SCC, squamous-cell carcinoma; Adeno, adenocarcinoma; Large, large-cell carcinoma; ND, not determined.

incidence of drug-related pneumonitis was 6.7% and was comparable to results of other studies.[23,24] Therefore, gefitinib monotherapy as a first-line treatment appears to be equally tolerable as a second-line treatment.

Thirteen of 22 patients who became resistant or were refractory to gefitinib monotherapy received salvage chemotherapy. The objective response rate was 30.8%, comparable to that of first-line chemotherapy. These results suggest that cancer cell populations that are sensitive to gefitinib might not be identical to those sensitive to chemotherapeutic drugs such as platinum agents or taxanes.

Somatic mutations in the tyrosine kinase domain of the *EGFR* gene were reported, and these mutations induced increased activity of *EGFR* and sensitivity to gefitinib in vitro and the predictive factor of response to gefitinib.[13,14] We evaluated *EGFR* gene status in 13 tumor samples and detected *EGFR* gene mutation in four tumors. Objective responses were achieved in two patients, but one patient showed PD whose tumor had a 15–base pair deletion mutation in exon 19. This suggested that response to gefitinib may not be determined by *EGFR* mutation in exon 19 or 21, and other mechanisms may relate to gefitinib resistance.

The detection of EGFR mutation from serum samples was carried out as a correlative study. These results provided us two major findings: (1) E746_A750del was detectable in serum sample obtained from NSCLC patients; and (2) E746_A750del was frequently observed in posttreatment serum samples obtained from the PR and SD patients.

It may be explained that DNA derived from destructive tumor cells that have responded to gefitinib may be more frequently observed in the circulating blood. Previous reports regarding detection of mutations in serum did not elucidate the changes in mutation status during treatment. We would like to do this in the next experiments to confirm our speculation. Our hypothesis is that serum detection of *EGFR* mutation will be a convenient means of predicting the sensitivity to gefitinib, although we could only demonstrate the feasibility of the *EGFR* mutation in serum in this report. We need to develop a highly sensitive methodology to improve the predictability of this assay.

In comparison of the mutation status of *EGFR* in actual tumors with serum DNA obtained from the same patients before treatment, 70% of patients who had sequence data obtained from both serum and tumor samples were conforming. Esteller et al. reported detection of aberrant promoter hypermethylation of tumor suppressor genes (*p16*, *DAP*, *GSTP1*, and *MGMT*) in serum DNA obtained from NSCLC patients and demonstrated that 73% of serum samples showed abnormal methylated DNA in the patients with the methylated primary tumors.[19] Another report investigating a point mutation of the *p53* gene and hypermethylation of *p16* in plasma DNA from breast cancer patients demonstrated that 66% of the patients with at least one molecular event in tumor DNA had some alteration in plasma DNA.[25] We believe that the sensitivity of our assay is equivalently sensitive to those of these previous reports.

CONCLUSION

In conclusion, 250 mg of oral gefitinib monotherapy as a first-line treatment produces obvious antitumor activity, with acceptable toxicities. Oral gefitinib monotherapy as a first-line treatment merits investigation in further clinical trials. Using serum samples from NSCLC patients, the *EGFR* mutation was detected. The detection of E746_A750del in the serum of untreated patients was not a predictor of gefitinib response in this study. However, further prospective studies using serum samples may be necessary to confirm this con-

clusion. The presence of *EGFR* mutation in serum may be a useful biomarker for monitoring gefitinib response.

ACKNOWLEDGMENTS

We thank the patients who enrolled into the trial and the investigators who enrolled them.

REFERENCES

1. Parkin DM, Bray F, Ferlay J, et al. Estimating the world cancer burden: Globocan 2000. *Int J Cancer* 2001;94:153–156.
2. Roskoski R Jr. The ErbB/HER receptor protein-tyrosine kinases and cancer. *Biochem Biophys Res Commun* 2004;319:1–11.
3. Scagliotti GV, Selvaggi G, Novello S, et al. The biology of epidermal growth factor receptor in lung cancer. *Clin Cancer Res* 2004; 10: 4227s–4232s.
4. Rusch V, Baselga J, Cordon-Cardo C, et al. Differential expression of the epidermal growth factor receptor and its ligands in primary non-small cell lung cancers and adjacent benign lung. *Cancer Res* 1993;53: 2379–2385.
5. Rusch V, Klimstra D, Venkatraman E, et al. Overexpression of the epidermal growth factor receptor and its ligand transforming growth factor alpha is frequent in resectable non-small cell lung cancer but does not predict tumor progression. *Clin Cancer Res* 1997;3:515–522.
6. Fontanini G, De Laurentiis M, Vignati S, et al. Evaluation of epidermal growth factor-related growth factors and receptors and of neoangiogenesis in completely resected stage I-IIIA non-small-cell lung cancer: amphiregulin and microvessel count are independent prognostic indicators of survival. *Clin Cancer Res* 1998;4:241–249.
7. Fukuoka M, Yano S, Giaccone G, et al. Multi-institutional randomized phase II trial of gefitinib for previously treated patients with advanced non-small-cell lung cancer. *J Clin Oncol* 2003;21:2237–2246.
8. Kris MG, Natale RB, Herbst RS, et al. Efficacy of gefitinib, an inhibitor of the epidermal growth factor receptor tyrosine kinase, in symptomatic patients with non-small cell lung cancer: a randomized trial. *JAMA* 2003;290:2149–2158.
9. Herbst RS, Giaccone G, Schiller JH, et al. Gefitinib in combination with paclitaxel and carboplatin in advanced non-small-cell lung cancer: a phase III trial—INTACT 2. *J Clin Oncol* 2004;22:785–794.
10. Giaccone G, Herbst RS, Manegold C, et al. Gefitinib in combination with gemcitabine and cisplatin in advanced non-small-cell lung cancer: a phase III trial—INTACT 1. *J Clin Oncol* 2004;22:777–784.
11. Thatcher N, Chang A, Parikh P, et al. Gefitinib plus best supportive care in previously treated patients with refractory advanced non-small-cell lung cancer: results from a randomised, placebo-controlled, multicentre study (Iressa Survival Evaluation in Lung Cancer). *Lancet* 2006;366: 1527–1537.
12. Johnson DH. Gefitinib (Iressa) trials in non-small cell lung cancer. *Lung Cancer* 2003; 41 (Suppl 1): S23–S28.
13. Lynch TJ, Bell DW, Sordella R, et al. Activating mutations in the epidermal growth factor receptor underlying responsiveness of non-small-cell lung cancer to gefitinib. *N Engl J Med* 2004;350:2129–2139.
14. Paez JG, Janne PA, Lee JC, et al. EGFR mutations in lung cancer: correlation with clinical response to gefitinib therapy. *Science* 2004;304: 1497–1500.
15. Pao W, Miller V, Zakowski M, et al. EGF receptor gene mutations are common in lung cancer from "never smokers" and are associated with sensitivity of tumors to gefitinib and elrotinib. *Proc Natl Acad Sci USA* 2004;101:13306–13311.
16. Shigematsu H, Lin L, Takahashi T, et al. Clinical and biological features associated with epidermal growth factor receptor gene mutations in lung cancers. *J Natl Cancer Inst* 2004;97:339–346.
17. Han SW, Kim TY, Hwang PG, et al. Predictive and prognostic impact of epidermal growth factor receptor mutation in non-small-cell lung cancer patients treated with gefitinib. *J Clin Oncol* 2006;23:2493–2501.
18. Sanchez-Cespedes M, Monzo M, Rosell R, et al. Detection of chromosome 3p alterations in serum DNA of non-small-cell lung cancer patients. *Ann Oncol* 1998;9:113–116.
19. Esteller M, Sanchez-Cespedes M, Rosell R, et al. Detection of aberrant promoter hypermethylation of tumor suppressor genes in serum DNA from non-small cell lung cancer patients. *Cancer Res* 1999;59:67–70.
20. Therasse P, Arbuck SG, Eisenhauer EA, et al. New guidelines to evaluate the response to treatment in solid tumors. European Organization for Research and Treatment of Cancer, National Cancer Institute of the United States, National Cancer Institute of Canada. *J Natl Cancer Inst* 2000;92:205–216.
21. Simon R. Optimal two-stage designs for phase II clinical trials. *Control Clin Trials* 1989;10:1–10.
22. Takano T, Ohe Y, Kusumoto M, et al. Risk factors for interstitial lung disease and predictive factors for tumor response in patients with advanced non-small cell lung cancer treated with gefitinib. *Lung Cancer* 2004;45:93–104.
23. Takeda K, Yamamoto N. An epidemiological survey for interstitial lung disease induced by gefitinib in patients with advanced non-small cell lung cancer. *Lung Cancer* 2003;41:S250.
24. Hotta K, Harita S, Bessho A, et al. Interstitial lung disease (ILD) during gefitinib treatment in Japanese patients with non-small cell lung cancer (NSCLC): Okayama Lung Cancer Study Group. *Proc Am Soc Clin Oncol* 2004;23:629.
25. Silva JM, Dominguez G, Garcia JM, et al. Presence of tumor DNA in plasma of breast cancer patients: clinicopathological correlations. *Cancer Res* 1999;59:3251–3256.

Breast Cancer Research and Treatment (2006) 99: 9–17
DOI 10.1007/s10549-006-9175-2

Gene expression profiling of ATP-binding cassette (ABC) transporters as a predictor of the pathologic response to neoadjuvant chemotherapy in breast cancer patients

Sarah Park[1,5], Chikako Shimizu[2], Tatsu Shimoyama[1], Masayuki Takeda[1], Masashi Ando[2], Tsutomu Kohno[2], Noriyuki Katsumata[2], Yoon-Koo Kang[5], Kazuto Nishio[1,3,4], and Yasuhiro Fujiwara[2]

[1]*Shien Lab, National Cancer Center Hospital, Tokyo, Japan;* [2]*Breast and Medical Oncology, National Cancer Center Hospital, Tokyo, Japan;* [3]*Pharmacology Division, National Cancer Center Research Institute, Tokyo, Japan;* [4]*Center for Medical Genomics, National Cancer Center Research Institute, Tokyo, Japan;* [5]*Division of Hematology–Oncology, Asan Medical center, University of Ulsan College of Medicine, Seoul, Korea*

Key words: ATP-binding-cassette (ABC) transporters, breast cancer, class prediction, neoadjuvant chemotherapy, oligonucleotide microarray

Summary

Drug resistance is a major obstacle to the successful chemotherapy. Several ATP-binding cassette (ABC) transporters including ABCB1, ABCC1 and ABCG2 have been known to be important mediators of chemoresistance. Using oligonucleotide microarrays (HG-U133 Plus 2.0; Affymetrix), we analyzed the ABC transporter gene expression profiles in breast cancer patients who underwent sequential weekly paclitaxel/FEC (5-fluorouracil, epirubicin and cyclophosphamide) neoadjuvant chemotherapy. We compared the ABC transporter expression profile between two classes of pretreatment tumor samples divided by the patients' pathological response to neoadjuvant chemotherapy (residual disease [RD] versus pathologic complete response [pCR]) ABCB3, ABCC7 and ABCF2 showed significantly high expression in the pCR. Several ABC transporters including ABCC5, ABCA12, ABCA1 ABCC13, ABCB6 and ABCC11 showed significantly increased expression in the RD ($p < 0.05$). We evaluated the feasibility of developing a multigene predictor model of pathologic response to neoadjuvant chemotherapy using gene expression profiles of ABC transporters. The prediction error was evaluated by leave-one-out cross-validation (LOOCV). A multigene predictor model with the ABC transporters differentially expressed between the two classes ($p \leq 0.003$) showed an average 92.8% of predictive accuracy (95% CI, 88.0–97.4%) with a 93.2% (95% CI, 85.2–100%) positive predictive value for pCR, a 93.6% (95% CI, 87.8–99.4%) negative predictive value, a sensitivity of 88.1%(95% CI, 76.8–99.4%), and a specificity of 95.9% (91.1% CI, 87.8–100%). Our results suggest that several ABC transporters in human breast cancer cells may affect the clinical response to neoadjuvant chemotherapy, and transcriptional profiling of these genes may be useful to predict the pathologic response to sequential weekly paclitaxel/FEC in breast cancer patients.

Introduction

Resistance to chemotherapy is a significant obstacle to appropriate treatment of cancer patients. Various cellular pathways may play a role in drug resistance and ATP-binding cassette (ABC) transporters are one of the most well known mediators leading to drug resistance and treatment failure. To date 49 ABC transporter genes have been identified and classified into seven groups, ABCA, ABCB, ABCC, ABCD, ABCE, ABCF, and ABCG (database of ABC transporters available at http://nutrigene.4t.com/humanabc.htm).

Extensive studies have been conducted on the individual proteins or genes of ABC transporter members regarding their role in chemoresistance. ABCB1 (MDR1-P-gp) [1,2], ABCC1 (MRP1) [3], and ABCG2 (MXR) [4] are particularly well known as mediators leading to resistance to several chemotherapeutic agents including paclitaxel [5], topoisomerase inhibitors [6], anthracyclin [7] and tyrosine kinase inhibitors [8]. Although little has been known about most of ABC transporter members, other members of this family sharing sequence and structural homology may play roles in absorption, distribution, and excretion of chemotherapeutic agents and probably influence the response to chemotherapy.

Recently, using ABC transporter gene expression profiling, studies on the relationship of drug resistance and ABC transporter were performed in cancer cell lines [9,10].

The characterization of the comprehensive expression of these genes in relation to the clinical response to chemotherapy may be useful to determine on an individual basis the patient's underlying risk and choose the optimal therapeutic regimen to which the individual cancer patient is most likely to respond. We studied the relationship between ABC transporter gene expression and the responsiveness to chemotherapy in early breast cancer patients who underwent sequential weekly paclitaxel/FEC (5-fluorouracil, epirubicin and cyclophosphamide) neoadjuvant chemotherapy and evaluated the feasibility of developing a multigene predictor model of pathologic response using differentially expressed ABC transporters on the basis of microarray data.

Materials and methods

Patient and sample preparation

This study was performed at the National Cancer Center Hospital, Tokyo, Japan. This study was approved by the institutional review boards of the National Cancer Center. Twenty-one pretreatment samples were obtained from breast cancer patients who underwent neoadjuvant chemotherapy from 2002 to 2004. All patients underwent pretreatment core needle biopsy (CNB) of the primary tumor tissue before starting neoadjuvant chemotherapy. The core needle biopsy was done using 14–16 gauge needles.

The patients received 4 cycles of FEC (5-Fluorouracil 500 mg/m^2, Epirubicin 100 mg/m^2 and Cyclophosphamide 500 mg/m^2) every three weeks followed by 12 cycles of weekly paclitaxel (80 mg/m^2). Additionally, in the case of HER2 positive determined by immunohistochemical staining (IHC), the specific inhibitory antibody of HER2 receptor, Trastuzumab (Herceptin®) was added in the course of the paclitaxel (Herceptin 4 mg/kg on day1 then 2 mg/kg weekly). Samples that showed 3+ IHC staining were considered as HER2 positive.

Every patient underwent surgery on the completion of the neoadjuvant chemotherapy, and histopathologic examination was performed. As described previously [11], pathologic complete response (pCR) was defined as no pathologic evidence of any residual invasive cancer cells in the breast and axillary lymph nodes, and residual disease (RD) was defined as any residual cancer cells on the histopathologic examination. Informed consent was obtained from all patients for voluntary participation in the study.

Tissue preparation and microarray

Samples for the microarray were collected into tubes containing Isogen (Nippon gene, Toyama) and stored at −80 °C. Total RNA was extracted by the single step method of Chomczynski et al. [12] with acid guanidinium thiocyanate phenol chloroform after homogenizing the tissue using a high speed homogenizer. The mean yield of RNA was 23.1 μg (ranged from 12.3 to 31.6 μg) from each collected samples. RNA that had distinct ribosomal RNA band by electrophoresis and had A_{260}/A_{280} absorbance ratio ranging from 1.8 to 2.1 was used for cDNA synthesis. Gene expression profiles were analyzed on a high-density oligonucleotide microarray (GeneChip® HG-U133 Plus 2.0; Affymetrix, Santa Clara, CA) containing 54,675 probe sets. The oligonucleotide microarray procedure for generation of the biotin-labeled cyclic RNA (cRNA) by *in vitro* transcription, hybridization to the array and scanning were performed according to the manufacturer's instructions. The amplification cycle of RNA to cDNA and cDNA to cRNA was performed using the GeneChip® 3′-Amplification Reagents One-Cycle cDNA Synthesis Kit including SuperScript II reverse transcriptase and a T7-$(dT)_{24}$ primer (Affymetrix). The synthesized cRNA was biotinylated using GeneChip 3′-amplification reagents for IVT labeling. The labeled cRNA was then purified and chemically fragmented at 94 °C for 35 min using the GeneChip Sample Cleanup Module (Affymetrix). The labeled fragmented cRNA was next hybridized to the GeneChip® at 45 °C for 16 h according to the manufacturer's instructions. The hybridized probe array was washed and stained with streptavidin-phycoerythrin. The stained probe array was scanned with a GeneChip® Scanner3000 (Affymetrix) at 570 nm. The signal intensity of the gene expression level was calculated by GeneChip Operating Software, Ver.1 (Affymetrix).

Data analysis

Microarray data analyses were performed with BRB ArrayTools developed by Dr. Richard Simon and Amy Peng Lam. (http://linus.nci.nih.gov/BRB-ArrayTools.html) which provides a variety of tools for the analysis of gene expression profile. Gene expression data were log transformed (base 2) and normalized to the median expression value of all genes on each array. Any genes in which the expression levels did not differ by at least by 1.5 fold from the median in at least 20% of the arrays were filtered out, for the exclusion of the genes showing minimal variation across the set of arrays. In addition, if an expression value was missing or filtered out in more than 50%, these data were excluded. The final data set included 50,508 clones, and contained all 49 ABC transporter genes. The list of transcripts on ABC transporters was obtained using GeneSprings software (http://www.silicongenetics.com/cgi/SiG.cgi/index.smf) from Agilent Technologies (Waldbronn, Germany). (Supplementary data).

Class comparison

To identify informative genes differentially expressed between the two classes of patients grouped by their pathologic response, we used supervised classification methods applying the random variance *t*-test to data using the BRB Array Tools and was accompanied by multivariate permutation tests in order to minimize false-positives with the maximum allowed number of

false positives set at 10, a false discovery rate of 0.1, and confidence 90%. Genes with a parametric p-value less than 0.05 were considered statistically significant.

Class prediction

To develop a prediction model of pathologic response using the ABC transporter gene expression profiles, we used the class prediction tools of BRB ArrayTools in which six multivariate classification methods were available including a compound covariate predictor [13], a K-nearest neighbor analysis ($K=1$, 3), a nearest centroid analysis, a support vector machine [14] and a diagonal linear discriminate analysis.

For the evaluation of the feasibility of developing a multigene predictor model of response to neoadjuvant chemotherapy using differentially expressed ABC transporters, six different multivariate classification models were examined. Firstly, we determined the number of genes that were included in the classifier model using a paired t-test applying multiple univariate parametric significance thresholds, and developed a classifier model based on these selected genes at the univariate parametric significance thresholds. With changes in the parametric significance thresholds, the multivariate classification algorithms were performed iteratively evaluating the classification error and the classifier p-value to identify the best classifier, and the processes were iteratively performed for each number of genes included in the classifier (determined by the significance threshold). The prediction error of each model was evaluated by leave-one-out cross-validation (LOOCV) [15]. This validation procedure was performed in a manner that removed the left-out sample before selecting the discriminate genes [15,16]. The classifier p-value, the probability that similar low error rate happen by chance, was obtained by a random permutation test performed 2000 times.

Results

The patient characteristics

All the patients received 4 courses of FEC (5-fluorouracil, epirubicin and cyclophosphamide) combination chemotherapy followed by 12 courses of weekly paclitaxel. In those patients who were HER-2 positive by IHC, Trastuzumab (Herceptin®) was added in the course of the treatment. We divided the patients into two groups from the results of the histopathologic examination performed after the completion of the neoadjuvant chemotherapy. Pathologic data were available for nineteen patients. Patients with no pathologic evidence of any residual invasive cancer cells in breast were classified as 'pCR', and if any residual cancer cells were found in the histopathologic study, these patients were classified as 'RD' group. Thirty-six point eight percent (7) of the nineteen patients showed no pathologic evidence of any residual invasive cancer cells in the breast and were classified as pCR and 63.2% (12) of patients were classified as RD.

Gene expression profiling of differentially expressed ABC transporters

Using gene expression data of the pretreatment tumor sample, we compared the ABC transporter gene expression profile between the two groups (RD versus pCR). A probe set on all of the 49 human ABC transporters genes known so far was contained in the microarray chip we used (HG-U133 Plus 2.0; Affymetrix). To identify differentially expressed ABC transporter genes potentially associated with the clinical response to neoadjuvant chemotherapy, a supervised class comparison analysis was performed. The random variance model t-test was used to discover differentially expressed genes and was accompanied by a multivariate 1000 permutation tests in order to minimize false-positives with the maximum allowed number of false positives set at 10, a false discovery rate of 0.1 and 90% confidence.

By comparing the average expression level of each transcript on ABC transporters between the two classes of patients, the median expression level in the RD group was 107.8 (range 15.8–6009.1) and 104.4 in the pCR group (range 17.9–5690.6). The median of fold difference (RD: pCR) of transcripts on the ABC transporters was 1.0, ranging from 0.3 to 7.6. Several ABC transporters showed prominently high expression at over 50 fold of the median value although the tumor samples were all from the pretreatment chemotherapy-naïve patients. The highest average expression level in the RD group, 6009.1, was observed in ABCC5 (AF146074, RD: pCR = 6009.1:2427.5, fold ratio 2.48) and the highest expression level in the pCR group, 5690.6, was observed in TAP1 (ABCB2, NM_000593, RD: pCR = 4551.4:5690.6, fold ratio 0.8), the transporter associated with antigen processing (Table 1).

The ABC transporters, which were significantly differentially expressed with a parametric p-value of less than 0.05, are listed in Table 2. Several transcripts (ABCC5, TAP2/ABCB3) selected overlapped for the microarray chip (HG-U133 Plus 2.0) containing 54,675 probe sets, more than 30,000 human transcripts were detected, derived from more than 20,000 loci within the human genome and some transcripts represented the same human gene.

ABC transporters, the expression of which in the RD group was significantly increased, included ABCC5 (fold ratio 2.48, $p=0.000368$), ABCA12 (fold ratio 7.64, $p=0.000795$), ABCA1 (fold ratio 3.30, $p=0.000859$), ABCC13 (fold ratio 7.54, $p=0.0194$), ABCB6 (fold ratio 2.17, $p=0.0271$), and ABCC11 (fold ratio 2.71, $p=0.0486$) (Table 2). These genes all showed over 2 fold increases in RD compared with pCR tumors. ABCC5 was recently reported to confer resistance to

Table 1. Clinical characteristics of the patients

	No. of patients
Age, years	
Median	51
Range	30–61
Menstruation status	
Pre menopause	12
Post menopause	7
TNM stage	
IIA	8
IIB	7
IIIA	2
IIIB	2
Histology	
Invasive ductal	17
Mixed ductal/lobular	
Invasive lobular	1
Invasive mucinous	1
Nuclear grade	
1	1
2	9
3	9
HER2 status	
HER2-positive	4
HER2-negative	15
ER status	
ER-positive*	5
ER-negative	14
Pathologic response	
Pathologic complete response	7
Residual disease	12
Treatment arm	
A[a]	15
B[b]	4

*Cases in which more than 10% of tumor cells stained positive for ER by IHC classified as ER positive.
[a]Treatment arm A; 4 courses of FEC* followed by 12 courses of weekly paclitaxel.
[b]Treatment arm B; 4 courses of FEC* followed by 12 courses of weekly paclitaxel with Trastuzumab.
*FEC combination chemotherapy (5-fluorouracil, epirubicin and cyclophosphamide).

5-fluorouracil [17] selected with the lowest p-value and it showed the highest gene expression level in tumors with decreased response. (AF146074, expression level RD: pCR = 6009.1: 2427.5, fold ratio 2.48).

CFTR (NM_000492, ABCC7, fold ratio 0.27, p= 0.007030), ABCF2 (NM_005692, fold ratio 0.32, p= 0.015901) and ABCB3 (M74447, TAP2, fold ratio 0.54, p= 0.019345), the transporter associated with antigen processing, showed increased expression in the pCR group but the biological significance concerning responsiveness to chemotherapy remains to be elucidated. The differentially expressed ABC transporter genes are shown in Figure 1 in hierarchical clustering view.

Development of multigene predictor model using the ABC transporter gene expression profile

To evaluate the feasibility of developing a multigene predictor model of response to neoadjuvant chemotherapy using the ABC transporter expression profile, six different multivariate classification models were examined.

Firstly, we determined the number of discriminate genes that were included in the classifier model by applying multiple univariate parametric significance thresholds, and developed a classifier model based on these selected genes at the significance thresholds. With changes in the parametric significance thresholds, the classification error and classifier p-value for each multivariate classification algorithms were evaluated iteratively by LOOCV (leave one out cross validation) [15] and the random permutation test to identify the best classifier model. The classifier p-value, the probability that a similar low error rate could happen by chance, was calculated by 2000 random permutation tests. We calculated the average of the classification error and the classifier p-value of six classifier models at each significance threshold. Figure 2 shows the change in the average classifier p-value for six multivariate classification models from the permutation test and the average of the classification error rate relative to multiple univariate parametric significance thresholds.

During this iterative process, the average estimated misclassification error and classifier p-value also dropped as the significance threshold decreased to 0.003, but applying further stringent significance thresholds caused a steep increase in the classification error. When the ABC transporters differentially expressed between the two classes at a significance threshold level of 0.003 were used for class prediction, the average of the classification error was minimal, 0.072 (92.8% of predictive accuracy, 95% CI, 88.0–97.4%), with the classifier p = 0.012, 93.2% (95% CI, 85.2–100%) positive predictive value for the pCR group, 93.6% (95% CI, 87.8–99.4%) negative predictive value, sensitivity for the pCR group 88.1% (95% CI, 76.8–99.4%), and a specificity of 95.9% (91.1% CI, 87.8–100%). The respective values for each model are represented in Table 3. On applying the compound covariate predictor classifier model, the predictive accuracy reached 100% with a classifier p-value of 0.0005. The ABC transporters selected as the best classifiers are presented in Table 4. The list included ABCA1, ABCA12 and ABCC5, recently reported to confer resistance to cyclic nucleotides including 5-fluorouracil [17].

Our results suggest that the ABC transporter genes expression pattern may be useful in predicting the pathologic response to sequential weekly paclitaxel/FEC in breast cancer patients.

Discussion

To determine the optimal therapeutic regimen to which the individual cancer patient is most likely to respond on

Table 2. Differentially expressed ABC transporters ordered by significance

Gene symbol	Genbank	Parametric *p*-value*	% CV support	RD[a]	pCR[b]	Fold difference[c]	Description
ABCC5	AF146074	0.000368	100	6009.1	2427.5	2.48	ABC, sub-family C (CFTR/MRP), member 5
ABCC5	BE550362	0.000463	100	3571.5	1234.4	2.89	ABC, sub-family C (CFTR/MRP), member 5
ABCA12	AL080207	0.000795	100	711.7	93.1	7.64	ABC, sub-family A (ABC1), member 12
ABCA1	AL833227	0.000859	100	166.8	50.5	3.3	ABC, sub-family A (ABC1), member 1
CFTR	NM_000492	0.007030	100	27.7	104.4	0.27	cystic fibrosis transmembrane conductance regulator, ABC (sub-family C, member 7)
ABCF2	NM_005692	0.015901	100	49.4	154.1	0.32	ABC, sub-family F (GCN20), member 2
TAP2	M74447	0.019345	89	543.4	1008.5	0.54	Transporter 2, ABC, sub-family B (MDR/TAP)
ABCC13	NM_172025	0.019377	100	157.5	20.9	7.54	ABC, sub-family C (CFTR/MRP), member 13
ABCB6	NM_005689	0.027077	89	1471.9	677.5	2.17	ABC, sub-family B (MDR/TAP), member 6
TAP2	AA573502	0.042069	58	1740.5	2802	0.62	Transporter 2, ABC, sub-family B (MDR/TAP)
ABCC11	AF352582	0.048626	42	160.9	59.4	2.71	ABC, sub-family C (CFTR/MRP), member 11

Table sorted by *p*-value. * *p* by random variance *t*-test.
[a]Geometric mean of intensities in the RD group.
[b]Geometric mean of intensities in the pCR group.
[c]Fold difference of geometric means RD: pCR.

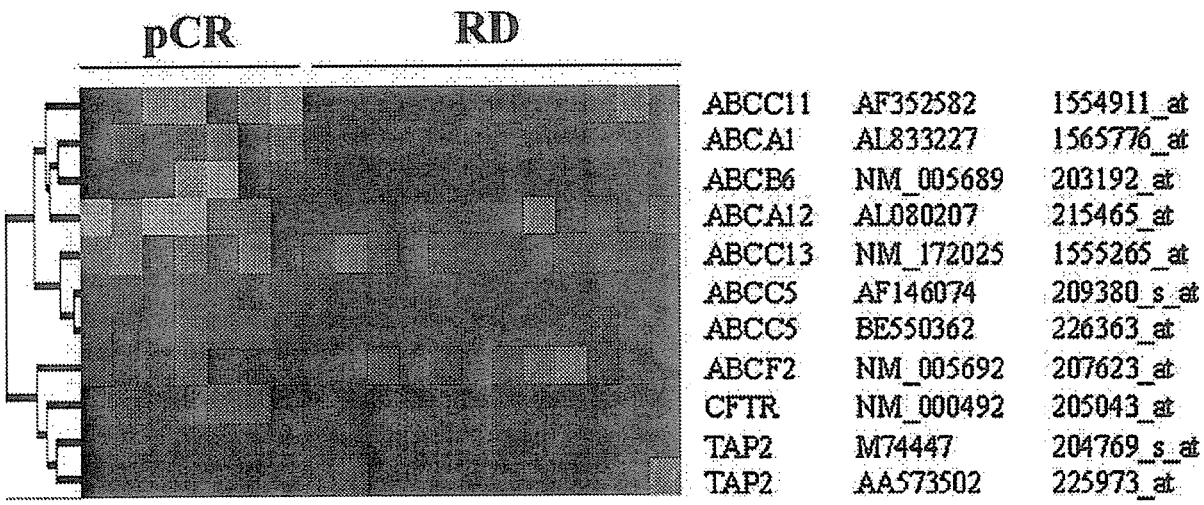

Figure 1. Hierarchical clustering of differentially expressed ABC transporters associated with the response to neoadjuvant chemotherapy in breast cancer patients. The cluster image map shows patterns of differential ABC transporter gene expression in breast cancer patients in respect to the response to neoadjuvant chemotherapy. The hierarchical clustering on each axis was performed using the complete linkage algorithm. Relatively highly expressed genes are shown in red, low expressed genes are shown in green.

an individual basis, there is a real need to develop an appropriate predictor to identify those cancer patients most likely to require or benefit from particular therapies. Resistance to chemotherapy is significant obstacle to appropriate treatment of cancer patients and affects the treatment outcome. Numerous cellular mechanisms exist which are responsible for the treatment failure due to chemoresistance. ABC transporters are the one of the major factors leading to drug resistance. Extensive study has been conducted on the ABC transporters, and ABCB1 (MDR1-P-gp) [1,2], ABCC1-MRP1 [3], and ABCG2-MXR [4] are particularly well known for their role in resistance to several chemotherapeutic agents. Because the members of the ABC transporters are grouped by sequence homology, the remained members may play roles in absorption, distribution, and excretion of chemotherapeutic agent and probably be related to drug resistance although little has been known about most of the functions of these genes. Characterization of the expression of the genes related to chemoresistance is an interesting subject and may lead to clinically useful predictors of response to chemotherapy. The profiling of ABC transporter genes in relation to the clinical response to chemotherapy may also be useful to determine the patient's underlying risk and choose the optimal therapeutic regimen to which the individual cancer patient is most likely to respond.

Focusing on the ABC transporters, we analyzed the gene expression profile in breast cancer patients using microarray data that contain the transcripts of all the

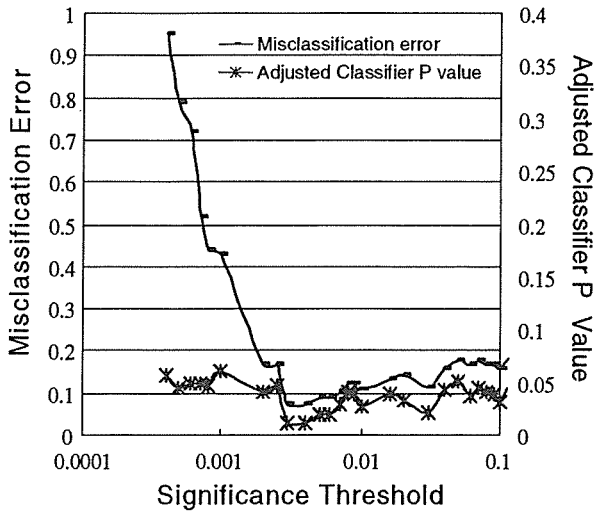

Figure 2. Multivariate predictive classification models in leave-one-out cross-validation and permutation test with an increasing significance threshold at which genes were selected as a classifier. The *x*-axis represents the significance threshold p value used to select the discriminate genes as classifiers. The *y*-axis shows the average of the misclassification error rate determined by leave-one-out cross-validation and the average classifier *p*-value, the probability that a similar low error rate could happen by chance calculated after 2000 permutations. Classifier genes selected as differentials between the 2 classes at a significance threshold $p = 0.003$ level showed the highest discriminate value.

members of ABC transporter family. We compared the expression pattern of the ABC transporters between two classes of pretreatment tumor samples divided by the pathologic response to neoadjuvant chemotherapy (RD versus pCR).

On microarray analysis, several ABC transporters showed differential expression between the two groups of tumors. Of interest, several ABC transporters showed increased expression in the pCR group, including CFTR (NM_000492, ABCC7, fold ratio 0.27, $p = 0.007030$), ABCF2 (NM_005692, fold ratio 0.32, $p = 0.015901$) and ABCB3 (M74447, TAP2, fold ratio 0.54, $p = 0.019345$). ABCB3 is known to be involved in antigen presenting by transporting peptides necessary for the assembly of major histocompatibility complex (MHC) class I molecules from the cytoplasm to the endoplasmic reticulum [18]. It is also known that its reduced expression is associated with HLA class I deficient human tumor cell lines [19] and it has been suggested that it is related to the aggressive features of some kinds of tumors [20–22]. Its increased expression has been found to be associated with pathological complete response in our clinical samples, but any clinical significance in the treatment of in breast cancer remains to be elucidated.

Five ABC transporters ABCC5 (AF146074, fold ratio 2.48, $p = 0.000368$), ABCA12 (AL080207, fold ratio 7.64,

Table 3. Performance of the multivariate classifier; the sensitivity, specificity, PPV and NPV for the pCR group of each predictor model at a significance threshold of $p = 0.003$

	CCV[a]	1NNC[b]	3NNC[c]	NCC[d]	SVM[e]	LDD[f]	Average[g]
Sensitivity	100	85.7	85.7	85.7	71.4	100	88.1
Specificity	100	91.7	91.7	100	100	91.7	95.9
PPV	100	85.7	85.7	100	100	87.5	93.2
NPV	100	91.7	91.7	92.3	85.7	100	93.6
Misclassification error	0	0.05	0.11	0.11	0.05	0.11	0.072
Percent correctly classified	100	95	89	89	95	89	92.8
Classifier P	5.00E-04	0.014	0.025	0.006	0.023	0.005	0.01225

[a]Compound covariate predictor classifier.
[b]1-Nearest neighbor classifier.
[c]3-Nearest neighbor classifier.
[d]Nearest centroid classifier.
[e]Support vector machine classifier.
[f]Linear diagonal discriminant analysis classifier.
[g]Average value of six multivariate classifier models.

Table 4. ABC transporters selected as best classifiers at a significance threshold of 0.003

Gene symbol	Genbank	*t*-Value	Parametric *p*-value*	% CV support	RD[a]	pCR[b]	§Fold difference	Description
ABCC5	AF146074	4.43	0.000368	100	6009.1	2427.5	2.48	ABC, sub-family C (CFTR/MRP), member 5
ABCC5	BE550362	4.32	0.000463	100	3571.5	1234.4	2.89	ABC, sub-family C (CFTR/MRP), member 5
ABCA12	AL080207	4.07	0.000795	100	711.7	93.1	7.64	ABC, sub-family A (ABC1), member 12
ABCA1	AL833227	4.04	0.000859	100	166.8	50.5	3.30	ABC, sub-family A (ABC1), member 1

Table sorted by *p* value.
*Parametric *p*-value by random variance *t*-test.
[a]Geometric mean of intensities in the RD group.
[b]Geometric mean of intensities in the pCR group. §Fold difference of geometric means; RD: pCR.

$p = 0.000795$), ABCA1 (AL833227, fold ratio 3.30, $p = 0.000859$), ABCC13 (NM_172025, fold ratio 7.54, $p = 0.0194$), ABCB6 (NM_005689, fold ratio 2.17, $p = 0.0271$) and ABCC11 (AF352582, fold ratio 2.71, $p = 0.0486$) showed significantly increased expression in the RD group associated with a decreased responsiveness to sequential weekly paclitaxel/FEC (5-fluorouracil, epirubicin and cyclophosphamide) neoadjuvant chemotherapy. Of these, ABCC5 was selected with the highest significance ($p = 0.000368$) and the highest expression level (RD: pCR 6009.1: 2427.5) although correlation between the gene expression level and the functional protein level remains to be seen. The ABCC5 (MRP5) transporter on human chromosome 3q27 has been known to be involved in the transport of nucleoside analogs [23] and has been reported to confer resistance to several drugs including methotrexate, GW1843 and ZD1694 (raltitrexed) [24]. Recently, Pratt et al. demonstrated that ABCC5 confers resistance against 5-fluorouracil [17] that was used in our neoadjuvant chemotherapy regimen. These results suggest that ABCC5 mediates transport of several chemotherapeutic agents and may contribute to resistance against 5-fluorouracil which is presently used in neoadjuvant chemotherapy.

In our clinical trial setting, ABCB1, known to confer resistance to several chemotherapeutic agents including paclitaxel, did not significantly increase in tumors with decreased response to neoadjuvant chemotherapy. Samples used in this study were all from chemotherapy-naïve patients and the time of exposure to the drug may not have been sufficient to induce the gene expression of this transporter. Although several ABC transporters showed high expression levels in the pretreatment samples, ABCB1 did not show significantly high expression. ABCB1 may thus play a greater role in resistance to chemotherapy in a secondary chemotherapy clinical setting than in first line chemotherapy when the exposure time is sufficiently long to induce the gene expression of the transporters known to be inducible by exposure to that chemotherapeutic agent [25,26].

But, some ABC transporters may also play significant role in chemoresistance in early breast cancer. Recently, it was reported that ABCC1 expression predict shorter relapse free survival and overall survival and play important role in resistance to chemotherapy in early breast cancer who underwent CMF (cyclophosphamide, methotrexate, and fluorouracil) adjuvant chemotherapy [27].

A variety of compounds are transported by ABC transporters through the lipid bilayer and still little has been known about the function of individual transporters in transport of chemotherapeutic agents. ABCA1 has been implicated in the control of the extrusion of membrane phospholipids and cholesterol toward specific extracellular acceptors [28] and macrophage interleukin-1 beta secretion and apoptosis [29]. ABCC13, highly expressed in the RD group mapped to chromosome 21q11.2 has been suggested that it might be associated with hematopoiesis. It has also been reported that ABCC13 shows decreased expression during cell differentiates [30]. ABCC11, called MRP8 is known to be a cyclic nucleotide efflux pump and a resistance factor for fluoropyrimidines 2′,3′-dideoxycytidine and 9′-(2′-phosphonylmethoxyethyl) adenine [31]. Szakacs et al. [10] suggested ABCC11 mediated resistance may not be confined to nucleoside analog, demonstrating that the ABCC11 transfected cell confers resistance to NSC 671136 by 2–3 fold. ABCB6 is a mitochondrial half transporter that is known to be involved in the transport of a precursor of the Fe/S cluster from mitochondria to the cytosol [32]. A recent report showed that several ABC transporters including ABCB6 amplified drug resistance in a non small cell lung cancer cell line (A549/CPT) in comparison with its parental cell [33].

Although the role in chemoresistant of individual transporters selected in our study to discriminate between the pCR and RD groups remains to be revealed, the transporters may also play roles in response to chemotherapy by influencing absorption, distribution, and excretion of chemotherapeutic agents.

To evaluate the predictive signature of ABC transporters, we examined multigene predictor model of response to neoadjuvant chemotherapy using differentially expressed ABC transporters. Six different multivariate classification models were examined. When the ABC transporters differentially expressed between the two classes at a significance threshold level of 0.003 were used for class prediction, an average 92.8% of predictive accuracy was observed, with a 93.2% positive predictive value for the pCR group, 93.6% negative predictive value, sensitivity for the pCR group of 88.1%, and 95.9% specificity. The classifier p-value, the probability that a similar low error rate could happen by chance, was also low ($p = 0.012$). The optimum classifier model included ABCC5, ABCA1, and ABCA12. These genes all showed high expression in tumors in the RD group.

Of interest, although we developed the class prediction model from a small subset of genes, i.e., genes belonging only to the ABC transporter family, the predictive accuracy reached above 90% with quite a low classifier p-value although these prediction models based on ABC transporter genes need to be validated in future studies by comparing the classification model with all subsets of genes and with larger numbers of samples.

Our result suggest that several ABC transporters in human breast cancer cells may contribute to the clinical response to neoadjuvant chemotherapy and gene expression profiling of these ABC transporters may be useful in prediction of the pathologic response to sequential weekly paclitaxel/FEC in breast cancer patients.

Acknowledgments

This work was partially supported by funds for the Third Term Comprehensive 10-Year Strategy for

Cancer Control and a Grant-in-Aid for Scientific Research and for Health and Labor Science Research Grants, Research on Advanced Medical Technology, H14-Toxico-007. We are grateful to Tokuzo Arao, Tsutomu Ohta, and Takayuki Kinoshita, for their contribution to the article and assistance in collection of clinical data. Analyses were carried out using BRB ArrayTools developed by Dr. Richard Simon and Amy Peng Lam.

References

1. Shen DW, Fojo A, Chin JE, Roninson IB, Richert N, Pastan I, Gottesman MM: Human multidrug-resistant cell lines: increased mdr1 expression can precede gene amplification. Science 232: 643–645, 1986
2. Roninson IB, Chin JE, Choi KG, Gros P, Housman DE, Fojo A, Shen DW, Gottesman MM, Pastan I: Isolation of human mdr DNA sequences amplified in multidrug-resistant KB carcinoma cells. Proc Natl Acad Sci USA 83: 4538–4542, 1986
3. Rosenberg MF, Mao Q, Holzenburg A, Ford RC, Deeley RG, Cole SP: The structure of the multidrug resistance protein 1 (MRP1/ABCC1). Crystallization and single-particle analysis. J Biol Chem 276: 16,076–16,082, 2001
4. Doyle LA, Yang W, Abruzzo LV, Krogmann T, Gao Y, Rishi AK, Ross DD: A multidrug resistance transporter from human MCF-7 breast cancer cells. Proc Natl Acad Sci USA 95: 15,665–15,670, 1998
5. Mechetner E, Kyshtoobayeva A, Zonis S, Kim H, Stroup R, Garcia R, Parker RJ, Fruehauf JP: Levels of multidrug resistance (MDR1) P-glycoprotein expression by human breast cancer correlate with in vitro resistance to taxol and doxorubicin. Clin Cancer Res 4: 389–398, 1998
6. Candeil L, Gourdier I, Peyron D, Vezzio N, Copois V, Bibeau F, Orsetti B, Scheffer GL, Ychou M, Khan QA, Pommier Y, Pau B, Martineau P, Del Rio M: ABCG2 overexpression in colon cancer cells resistant to SN38 and in irinotecan-treated metastases. Int J Cancer 109: 848–854, 2004
7. Salmon SE, Grogan TM, Miller T, Scheper R, Dalton WS: Prediction of doxorubicin resistance in vitro in myeloma, lymphoma, and breast cancer by P-glycoprotein staining. J Natl Cancer Inst 81: 696–701, 1989
8. Nakamura Y, Oka M, Soda H, Shiozawa K, Yoshikawa M, Itoh A, Ikegami Y, Tsurutani J, Nakatomi K, Kitazaki T, Doi S, Yoshida H, Kohno S: Gefitinib ("Iressa", ZD1839), an epidermal growth factor receptor tyrosine kinase inhibitor, reverses breast cancer resistance protein/ABCG2-mediated drug resistance. Cancer Res 65: 1541–1546, 2005
9. Gillet JP, Efferth T, Steinbach D, Hamels J, de Longueville F, Bertholet V, Remacle J: Microarray-based detection of multidrug resistance in human tumor cells by expression profiling of ATP-binding cassette transporter genes. Cancer Res 64: 8987–8993, 2004
10. Szakacs G, Annereau JP, Lababidi S, Shankavaram U, Arciello A, Bussey KJ, Reinhold W, Guo Y, Kruh GD, Reimers M, Weinstein JN, Gottesman MM: Predicting drug sensitivity and resistance: profiling ABC transporter genes in cancer cells. Cancer Cell 6: 129–137, 2004
11. Wolmark N, Wang J, Mamounas E, Bryant J, Fisher B: Preoperative chemotherapy in patients with operable breast cancer: nine-year results from National Surgical Adjuvant Breast and Bowel Project B-18. J Natl Cancer Inst Monogr: 96–102, 2001
12. Chomczynski P, Sacchi N: Single-step method of RNA isolation by acid guanidinium thiocyanate–phenol–chloroform extraction. Anal Biochem 162: 156–159, 1987
13. Radmacher MD, McShane LM, Simon R: A paradigm for class prediction using gene expression profiles. J Comput Biol 9: 505–511, 2002
14. Ramaswamy S, Tamayo P, Rifkin R, Mukherjee S, Yeang CH, Angelo M, Ladd C, Reich M, Latulippe E, Mesirov JP, Poggio T, Gerald W, Loda M, Lander ES, Golub TR: Multiclass cancer diagnosis using tumor gene expression signatures. Proc Natl Acad Sci USA 98: 15,149–15,154, 2001
15. Simon R, Radmacher MD, Dobbin K, McShane LM: Pitfalls in the use of DNA microarray data for diagnostic and prognostic classification. J Natl Cancer Inst 95: 14–18, 2003
16. Ambroise C, McLachlan GJ: Selection bias in gene extraction on the basis of microarray gene-expression data. Proc Natl Acad Sci USA 99: 6562–6566, 2002
17. Pratt S, Shepard RL, Kandasamy RA, Johnston PA, Perry W, III, Dantzig AH: The multidrug resistance protein 5 (ABCC5) confers resistance to 5-fluorouracil and transports its monophosphorylated metabolites. Mol Cancer Ther 4: 855–863, 2005
18. Momburg F, Hammerling GJ: Generation and TAP-mediated transport of peptides for major histocompatibility complex class I molecules. Adv Immunol 68: 191–256, 1998
19. Singal DP, Ye M, Ni J, Snider DP: Markedly decreased expression of TAP1 and LMP2 genes in HLA class I-deficient human tumor cell lines. Immunol Lett 50: 149–154, 1996
20. Meissner M, Reichert TE, Kunkel M, Gooding W, Whiteside TL, Ferrone S, Seliger B: Defects in the human leukocyte antigen class I antigen processing machinery in head and neck squamous cell carcinoma: association with clinical outcome. Clin Cancer Res 11: 2552–2560, 2005
21. Cresswell AC, Sisley K, Laws D, Parsons MA, Rennie IG, Murray AK: Reduced expression of TAP-1 and TAP-2 in posterior uveal melanoma is associated with progression to metastatic disease. Melanoma Res 11: 275–281, 2001
22. Atkins D, Breuckmann A, Schmahl GE, Binner P, Ferrone S, Krummenauer F, Storkel S, Seliger B: MHC class I antigen processing pathway defects, ras mutations and disease stage in colorectal carcinoma. Int J Cancer 109: 265–273, 2004
23. Allikmets R, Gerrard B, Hutchinson A, Dean M: Characterization of the human ABC superfamily: isolation and mapping of 21 new genes using the expressed sequence tags database. Hum Mol Genet 5: 1649–1655, 1996
24. Wielinga P, Hooijberg JH, Gunnarsdottir S, Kathmann I, Reid G, Zelcer N, van der Born K, de Haas M, van der Heijden I, Kaspers G, Wijnholds J, Jansen G, Peters G, Borst P: The human multidrug resistance protein MRP5 transports folates and can mediate cellular resistance against antifolates. Cancer Res 65: 4425–4430, 2005
25. Hu XF, Slater A, Rischin D, Kantharidis P, Parkin JD, Zalcberg J: Induction of MDR1 gene expression by anthracycline analogues in a human drug resistant leukaemia cellline. Br J Cancer 79: 831–837, 1999
26. Mealey KL, Barhoumi R, Burghardt RC, Safe S, Kochevar DT: Doxycycline induces expression of P glycoprotein in MCF-7 breast carcinoma cells. Antimicrob Agents Chemother 46: 755–761, 2002
27. Filipits M, Pohl G, Rudas M, Dietze O, Lax S, Grill R, Pirker R, Zielinski CC, Hausmaninger H, Kubista E, Samonigg H, Jakesz R: Clinical role of multidrug resistance protein 1 expression in chemotherapy resistance in early-stage breast cancer: the Austrian Breast and Colorectal Cancer Study Group. J Clin Oncol 23: 1161–1168, 2005
28. Schmitz G, Langmann T: Structure, function and regulation of the ABC1 gene product. Curr Opin Lipidol 12: 129–140, 2001
29. Schmitz G, Kaminski WE, Porsch-Ozcurumez M, Klucken J, Orso E, Bodzioch M, Buchler C, Drobnik W: ATP-binding cassette transporter A1 (ABCA1) in macrophages: a dual function in inflammation and lipid metabolism?. Pathobiology 67: 236–240, 1999
30. Yabuuchi H, Takayanagi S, Yoshinaga K, Taniguchi N, Aburatani H, Ishikawa T: ABCC13, an unusual truncated ABC transporter, is highly expressed in fetal human liver. Biochem Biophys Res Commun 299: 410–417, 2002
31. Guo Y, Kotova E, Chen ZS, Lee K, Hopper-Borge E, Belinsky MG, Kruh GD: MRP8, ATP-binding cassette C11 (ABCC11), is a cyclic nucleotide efflux pump and a resistance factor for

fluoropyrimidines 2′,3′-dideoxycytidine and 9′-(2′-phosphonylmethoxyethyl)adenine. J Biol Chem 278: 29,509–29,514, 2003
32. Mitsuhashi N, Miki T, Senbongi H, Yokoi N, Yano H, Miyazaki M, Nakajima N, Iwanaga T, Yokoyama Y, Shibata T, Seino S: MTABC3, a novel mitochondrial ATP-binding cassette protein involved in iron homeostasis. J Biol Chem 275: 17,536–17,540, 2000
33. Yasui K, Mihara S, Zhao C, Okamoto H, Saito-Ohara F, Tomida A, Funato T, Yokomizo A, Naito S, Imoto I, Tsuruo T, Inazawa J: Alteration in copy numbers of genes as a mechanism for acquired drug resistance. Cancer Res 64: 1403–1410, 2004

Address for offprints and correspondence: Kazuto Nishio, Shien Lab, National Cancer Center Hospital, Tsukiji 5-1-1, Chuo-ku, 104-0045, Tokyo, Japan; *Tel.:* +81-3-3542-6143; *Fax:* +81-3-3547-5185; *E-mail:* knishio@gan2.res.ncc.go.jp

Lung Cancer (2006) 53, 13–21

available at www.sciencedirect.com

SCIENCE DIRECT®

journal homepage: www.elsevier.com/locate/lungcan

Effects of different combinations of gefitinib and irinotecan in lung cancer cell lines expressing wild or deletional EGFR

Tatsu Shimoyama[a,b], Fumiaki Koizumi[a], Hisao Fukumoto[a], Katsuyuki Kiura[b], Mitsune Tanimoto[b], Nagahiro Saijo[a], Kazuto Nishio[a,*]

[a] *Shien-Lab and Medical Oncology, National Cancer Center Hospital, Pharmacology Division, National Cancer Center Research Institute, Tsukiji 5-1-1, Chuo-ku, Tokyo 104-0045, Japan*
[b] *Department of Medicine II, Okayama University Medical School, 2-5-1 Shikata-cho, Okayama 700-8558, Japan*

Received 8 November 2005; accepted 1 March 2006

KEYWORDS
Gefitinib;
CPT-11;
SN-38;
EGFR;
Combination;
Lung cancer

Summary EGFR mutations are a major determinant of lung tumor response to gefitinib, an EGFR-specific tyrosine kinase inhibitor. Obtaining a response from lung tumors expressing wild-type EGFR is a major obstacle. The combination of gefitinib and cytotoxic drugs is one strategy against lung cancers expressing wild-type EGFR. The DNA topoisomerase inhibitor irinotecan sulfate (CPT-11) is active against lung cancer. We examined the sensitivity of lung cancers expressing wild- or mutant-type EGFR to the combination of gefitinib and CPT-11. The in vitro effect of gefitinib and SN-38 (the active metabolite of CPT-11) was examined in seven lung cancer cell lines using the dye formation assay with a combination index. When administered concurrently, gefitinib and SN-38 had a synergistic effect in five of the seven cell lines expressing wild-type EGFR, whereas the combination was antagonistic in PC-9 cells and a PC-9 subline resistant to gefitinib and expressing deletional mutant EGFR (PC-9/ZD). When administered sequentially, treatment with SN-38 followed by gefitinib had remarkable synergistic effects in the PC-9 and PC-9/ZD cells. In an in vivo tumor-bearing model, this combination had a schedule-dependent synergistic effect in the PC-9 and PC-9/ZD cells. An immunohistochemical analysis of the tumors in mice treated with CPT-11 and gefitinib demonstrated that the number of Ki-67 positive tumor cells induced by CPT-11 treatment was decreased when CPT-11 was administered in combination with gefitinib. In conclusion, the sequential combination of CPT-11 and gefitinib is considered to be active against lung cancer.

1. Introduction

Lung cancer is one of the leading causes of cancer-related death, despite the use of conventional chemotherapy regi-

* Corresponding author at: Tel.: +81 3 3542 2511; fax: +81 3 3547 5185.
E-mail address: knishio@gan2.res.ncc.go.jp (K. Nishio).

0169-5002/$ – see front matter © 2006 Elsevier Ireland Ltd. All rights reserved.
doi:10.1016/j.lungcan.2006.03.014

mens. The epidermal growth factor receptor (EGFR) is frequently expressed in non-small cell lung cancer (NSCLC) and is correlated with a poor prognosis. Gefitinib ('Iressa') is an orally active, selective EGFR-tyrosine kinase inhibitor that blocks signal transduction pathways. Its clinical efficacy has been show in refractory NCSLC patients, but the survival benefit of this agent remains unclear. EGFR mutations have been identified in NSCLC, and lung cancers carrying the EGFR mutation have been reported to be hyperresponsive to gefitinib [1,2]. Mutant EGFR is a major determinant of lung tumor response to gefitinib, but the hyperresponsiveness of tumors expressing mutant EGFR has been observed in a small population. Now, obtaining a clinical benefit in lung tumors expressing wild-ype EGFR is a major obstacle. The combination of gefitinib and cytotoxic drugs is one strategy against lung cancers expressing wild-type EGFR. The DNA topoisomerase I inhibitor irinotecan (CPT-11) is a key drug in the treatment of patients with lung cancer and has been shown to prolong survival. SN-38 is the active metabolite of CPT-11 in vitro. The objective of this study was to determine the potential therapeutic utility of gefitinib when combined with CPT-11 therapy to lung cancer cell according to the treatment schedule and EGFR status.

Acquired resistance to gefitinib is also of clinical interest. Recently, Kobayashi et al. [3] reported that an EGFR mutation was related to the development of acquired resistance to gefitinib. We have established subclone PC-9/ZD cells that are resistant to gefitinib [4]. Our results suggested that another mechanism of resistance was active in PC-9/ZD cells. The effect of the combination of gefitinib and SN-38 in these PC-9/ZD cells was also examined.

2. Materials and methods

2.1. Drugs and chemicals

Gefitinib (*N*-(3-chloro-4-fluorophenyl)-7-methoxy-6-[3-(morpholin-4-yl)propoxy]quinazolin-4-amine) was provided by AstraZeneca (Cheshire, UK). Gefitinib was dissolved in dimethyl sulfoxide (DMSO) for the in vitro study. CPT-11 and SN-38 were obtained from Yakult Honsha (Tokyo, Japan) and were dissolved in dimethyl sulfoxide (DMSO) for both of the in vitro studies.

2.2. Cells and cultures

Human NSCLC cell lines PC-9, PC-7, and PC-14 derived from untreated patients with pulmonary adenocarcinoma were provided by Professor Y. Hayata, Tokyo Medical College. A small cell lung cancer cell line, H69, was established at the National Cancer Institute (Bethesda, MD, USA). The gefitinib-resistant subline, PC-9/ZD, was established from intrinsic hypersensitive cell PC-9 [5] in our laboratory [4]. A small cell lung cancer cell line, SBC-3, and an adenocarcinoma cell line, A549, were obtained from the Japanese Cancer Research Resources Bank (Tokyo, Japan). All cell lines were maintained in RPMI1640 (Nikken Bio Med. Lab., Kyoto, Japan) supplemented with 10% heat-inactivated fetal calf serum, 100 μg/ml streptomycin, and 100 units/ml penicillin in an incubator at 37 °C and 100% humidity in 5% CO_2 and air, as described previously [6].

2.3. RT-PCR

Specific primers designed for EGFR CDS were used to detect the EGFR mRNA, as described elsewhere [1]. Sixteen first-strand cDNAs were synthesized from the cells' RNA using an RNA PCR Kit (TaKaRa Biomedicals, Ohtsu, Japan). After the reverse transcription of 1 μg of total RNA with Oligo(dT)-M4 adaptor primer, the whole mixture was used for PCR with two oligonucleotide primers (5′-AATGTGAGCAGAGGCAGGGA-3′ and 5′-GGCTTGGTTTGGAGCTTCTC-3). PCR was performed with an initial denaturation at 94 °C for 2 min and 25 cycles of amplification (denaturation at 94 °C for 30 s, annealing at 55 °C for 60 s, and extension at 72 °C for 105 s).

2.4. Western blot analysis

The cultured cells were washed twice with ice-cold phosphate buffered saline (PBS), lysate in EBC buffer (50 mM Tris–HCl, pH 8.0; 120 mM NaCl; 0.5% Nonidet P-40; 100 mM NaF; 200 mM Na orthovanadate; and 10 mg/ml each of leupeptin, aprotinin and phenylmethylsulfonyl fluoride). The lysate was cleared by centrifugation at 20,000 × *g* for 5 min, and the protein concentration of the supernatant was measured using a BCA protein assay (Pierce, Rockford, IL, USA). For immunoblotting, 20 μg samples of protein were electrophoretically separated on a 7.5% SDS-polyacrylamide gel and transferred to a polyvinylidene difluoride (PVDF) membrane (Millipore, Bedford, MA, USA). The membrane was then probed with rabbit polyclonal antibodies against EGFR, HER2/neu, Her3 and Her4 (Santa Cruz Biotech, Santa Cruz, CA, USA) and phospho-EGFR specific for Tyr 845, Tyr 1045, and Tyr 1068 (numbers 2231, 2235 and 2234; Cell Signaling, Beverly, MA, USA).

2.5. Growth-inhibition assay

We used the tetrazolium dye (3,(4,5-dimethyl-2-thiazolyl)-2,5-diphenyl-2H-tetrazolium bromide, MTT) assay to evaluate the cytotoxicity of various drug concentrations. After incubation for 72 h at 37 °C, 20 μl of MTT solution (5 mg/ml in PBS) was added to each well; the plates were then incubated for a further 4 h at 37 °C. After centrifuging the plates at 200 × *g* for 5 min, the medium was aspirated from each well and 180 μl of dimethylsulfoxide was added to each well to dissolve the formazan. Optical density was measured at 562 and 630 nm using a Delta Soft ELISA analysis program interfaced with a Bio-Tek Microplate Reader (EL-340; Bio-Metallics, Princeton, NJ, USA). Each experiment was performed in six replicate wells for each drug concentration and was independently performed three or four times. The IC_{50} value was defined as the concentration needed for a 50% reduction in the absorbance, as calculated based on the survival curves. Percent survival was calculated as follows:

$$\frac{\text{Mean absorbance of six replicate wells containing drugs} - \text{mean absorbance of six replicate background wells}}{\text{mean absorbance of six replicate drug-free wells} - \text{mean absorbance of six replicate background wells}} \times 100.$$

2.6. Combined effect of gefitinib and SN-38 in vitro

After 24 h of incubation, gefitinib and SN-38 were added to each cell line according to one of the two combination schedules. For the concurrent schedule, gefitinib and SN-38 were added concurrently and were then incubated under the same conditions for 72 h. For the sequential schedule, gefitinib or SN-38 were added sequentially and were then incubated under the same conditions for 72 h. The combined effect of gefitinib and SN-38 on lung cancer cell growth was evaluated using a combination index (CI) [7]. The CI was produced using CalcuSym software (Biosoft, NY, USA). For any given drug combination, the CI represents the degree of synergy, additivity, or antagonism. CI was expressed in terms of fraction-affected (F_a) values, which represents the percentage of cells killed or inhibited by the drug. Using mutually exclusive ($\alpha = 0$) or mutually non-exclusive ($\alpha = 1$) isobologram equations, the F_a/CI plots for each cell line were constructed by computer analysis of the data generated from the median effect analysis. The CI values were interpreted as follows: <1.0 = synergism; 1.0 = additive; >1.0 = antagonism.

2.7. In vivo growth-inhibition assay

Experiments were performed in accordance with the United Kingdom Coordinating Committee on Cancer Research Guidelines for the welfare of animals with experimental neoplasia (second edition). Fig. 2A shows the treatment schedule. For the in vivo experiments, the combined therapeutic effect of orally or intraperitoneally administered gefitinib and intravenously injected CPT-11 was evaluated according to a predetermined schedule. The dose of each drug was set based on the results of a preliminary experiment involving the administration of each drug alone. Ten days before administration, PC-9 and PC-9/ZD cells were injected subcutaneously into the backs of the mice. Six mice per group were injected with tumor cells. Tumor-bearing mice were given either gefitinib (40 mg/kg/day, p.o.) on days 2–6, CPT-11 (50 mg/kg/day, i.v.) on day 1, both, or a placebo (5%(w/v) glucose solution). Alternatively, tumor-bearing mice were given gefitinib on days 2–6 and CPT-1 on days 2. The diameters of the tumors were measured using calipers on days 1, 5, 8, 12, 15 and 20 to evaluate the effects of treatment, and tumor volume was determined using the following equation: tumor volume $ab^2/2$ (mm^3) (where a is the largest diameter of the tumor and b is the shortest diameter). Day 20 denotes the day on which the effects of the drugs were estimated, and day "0" denotes the first day of treatment. All mice were sacrificed on day 20 after their tumors had been measured.

2.8. Immunohistochemistry

The tumors were harvested from the mice at the time of sacrifice. For hematoxylin-eosin (HE) and anti-CD31 and Ki-67 staining, the resected tumors were fixed in zinc-buffered formalin (Shandon Lipshaw, Pittsburgh, PA) overnight at 4 °C. After paraffin embedding and sectioning at 6 μm, formalin-fixed sections were stained with Mayer's H&E (Richard Allen, Kalamazoo, MI, USA). For anti-Ki-67 and anti-CD31 immunohistochemistry, the slides were heated in a water bath at 95–99 °C in Target Retrieval Solution (DAKO, Carpinteria, CA, USA) for 20 min, followed by a 20-min cool-down period at room temperature. After heat retrieval, the sections were rinsed well in PBS and stained with rabbit antihuman Ki-67 antigen (DAKO N-series, ready to use) or rat antimouse CD-31 antibody (BD PharMingen, Tokyo, Japan) according to the manufacturer's instructions and then were lightly counterstained with Mayer's hematoxylin. The sections were finally stained with an in situ Death Detection POD Kit (Roche Diagnostic GmbH, Mannheim, Germany), according to the manufacturer's instructions.

TUNEL staining was performed using the Apoptosis Detection System, Fluorescein (Promega, Madison, WI, USA). Briefly, 6-μm cryostat sections were fixed in 4% paraformaldehyde for 10 min at room temperature and rinsed in PBS with 0.1% Triton X-100. The sections were then incubated in Equilibration Buffer for 5 min at room temperature followed by incubation in TUNEL Mix, prepared according to the manufacturer's instructions, for 1 h at 37 °C. After successive washes in PBS, the sections were coverslipped using an antifade reagent.

Microvessel density was determined by calculating the proportion of CD31-positive cells. The Proliferation Index was determined by Ki-67 immunostaining and calculating the population of Ki-67-positive cells in five fields at 200×. The Apoptosis Index, determined by TUNEL staining, was calculated from the population of TUNEL-positive cells in five fields at 200×. The apoptosis:proliferation ratio equals the apoptosis index/proliferation index × 100. At least 1000 tumor cell nuclei from the most evenly and distinctly labeled areas were examined in each examination.

At least 1000 cancer cells were counted and scored per slide. Both the percentage of specifically stained cells and the intensity of immunostaining were recorded. Blood vessels were detected with an anti-von Willebrand factor (vWF) antibody (Chemicon). Microvessel density was determined by calculating the proportion of vWF-positive cells.

3. Results

3.1. Expression of Her-receptors and cellular sensitivity to gefitinib or SN-38 in lung cancer cell lines

The expression levels of EGFR in seven lung cancer cell lines were examined using RT-PCR with a primer set for exon 20 in EGFR. PC-14, SBC-3, H69, PC-7, and A549 cells showed a 570-bp-long PCR amplified product exhibiting wild-type EGFR mRNA (data not shown). On the other hand, a smaller PCR product was also detected in the PC-9 and PC-9/ZD cells, and this band was confirmed to be an in-frame 15-base deletion of exon 20 (E746_A750del).

We examined the protein levels of EGFR, Her2, Her3, and Her4 in the lung cell lines using immunoblotting. The quantitative data obtained by densitometorical analysis is summarized in Table 1. The protein levels of EGFR, Her2, and Her3 in the PC-9 cells were one- to four-fold higher than those in the other cell lines (PC-7, H69, PC-14, A549, and SBC-3).

Table 1 Comparison of Her family protein levels and gefitinib- and SN-38-induced growth inhibition

Cell lines	Relative expression[a]				Growth inhibition[b], $IC_{50} \pm S.D.$	
	EGFR	Her2	Her3	Her4	Gefitinib (μM)	SN-38 (nM)
PC-9	2.8[c]	3.2	3.7	ND	0.047 ± 0.061	8.09 ± 1.9
PC-9/ZD	1.6[c]	2.6	3.8	ND	7.7 ± 0.5	38.9 ± 7.0
PC-14	1.5	2.8	1.1	ND	17.1 ± 0.8	42.1 ± 2.6
SBC-3	2.4	2.6	1.0	ND	19.9 ± 5.4	1.07 ± 0.1
A549	2.3	2.3	1.4	ND	30.2 ± 2.2	293 ± 64.5
H69	1.3	1.3	2.0	ND	56.5 ± 3.2	27.2 ± 4.1
PC-7	1.0	1.0	1.2	ND	68.8 ± 14.8	20.5 ± 8.2

The IC_{50} value (μM) of each drug was measured by MTT assay, as described in Section 2. Each value is the mean ± S.D. of three or four independent experiments.

[a] Protein expression levels were analyzed by Western blotting.

[b] Drug concentration responsible for 50% growth inhibition in MTT assay at 72 h, calculated data for at least three dependent experiments.

[c] 15-base deletion EGFR, ND: not determined.

3.2. Cellular sensitivity of lung cancer cells to gefitinib and SN-38

The growth inhibitory effect of gefitinib and SN-38 on lung cancer cells was examined using an MTT assay. The IC_{50} values of gefitinib for the cell lines ranged from 46 nM (PC-9 cells) to 68 μM (PC-7 cells). The PC-9/ZD cells were ~200-fold resistant to gefitinib, compared with the parental PC-9 cells. Cellular sensitivity to gefitinib and the expression levels of EGFR and Her2 were negatively correlated with the IC_{50} values of gefitinib (Table 1). The IC_{50} values of SN-38 for these cell lines ranged from 1 nM (SBC-3) to 300 nM (A549). The range of sensitivity to gefitinib was wider than that to SN-38. No correlation in cellular sensitivity to gefitinib and SN-38 was seen.

3.3. In vitro combined effect of gefitinib and SN-38 on lung cancer cell lines

To evaluate the potential combined effect of gefitinib and SN-38, the combination index was determined using an MTT assay. The combined effects of gefitinib and SN-38 under the concurrent schedule are shown in Fig. 1. CI values of <1, >1, and 1 indicate a supra-additive effect (synergism), an antagonistic effect, and an additive effect, respectively. An additive to supra-additive growth-inhibitory effect was observed for all doses of gefitinib and SN-38 tested in cell lines expressing wild-type EGFR. On the other hand, a high CI index was observed in PC-9 cells and PC-9/ZD cells expressing mutant EGFR over a wide range of inhibition levels. These results suggest that gefitinib and SN-38 are synergistic in lung cancer cells expressing wild-type EGFR but not in cell lines expressing mutant EGFR in vitro.

3.4. Schedule-dependent synergy of gefitinib and SN-38 in lung cancer cells

Next, we examined the schedule dependency of the combined effects of gefitinib and SN-38 in the cell lines. The five cell lines expressing wild-type EGFR showed synergistic (PC-14, H69, and A549 cells) or additive effects (SBC-3 and PC-7 cells) for all three schedules: concurrent administration, SN-38 followed by gefitinib administration, and gefitinib followed by SN-38 administration (Fig. 1A). In the PC-9 cells, concurrent administration and gefitinib followed by SN-38 administration were antagonistic, but SN-38 followed by gefitinib administration was synergistic (Fig. 1B). In the PC-9/ZD cells, concurrent administration was antagonistic, but sequential administration was synergistic. These schedule-dependent combined effects were observed in the cells expressing mutant EGFR.

3.5. Combined effects of gefitinib and SN-38 in vivo

To estimate the schedule-dependent effects in vivo, nude mice bearing tumors were treated with gefitinib and CPT-11 according to sequential or concurrent schedules (Fig. 2A). Mice bearing PC-14 tumors were treated with gefitinib and CPT-11 according to sequential or concurrent schedules. CPT-11 (50 mg/kg) alone potentially reduced the tumor size, and the combination of gefitinib and CPT-11 was synergistic. In particular, the administration of CPT-11 followed by gefitinib cured the mice bearing PC-14 cells (Fig. 2B).

Mice bearing PC-9 or PC-9/ZD tumors were treated with gefitinib and CPT-11 according to sequential or concurrent schedules. Gefitinib (40 mg/kg) alone potentially reduced the PC-9 tumors, and CPT-11 (50 mg/kg) followed by gefitinib administration reduced the tumor size of PC-9 xenografts more dramatically (gefitinib alone: $P=0.012$, sequential combination: $P=0.005$) (Fig. 2B). On the other hand, the concurrent schedule produced an antagonistic effect. Body weight loss was not observed in any of the mice treated according to the above schedules (Fig. 2C). CPT-11 followed by gefitinib administration is a potentially beneficial schedule against PC-9 and PC-9/ZD cells expressing mutational EGFR. The results of these in vivo experiments were consistent with those of the in vitro studies.

To elucidate the synergistic mechanisms of CPT-11 and gefitinib in vivo, tumor samples of the PC-9 and PC-9/ZD

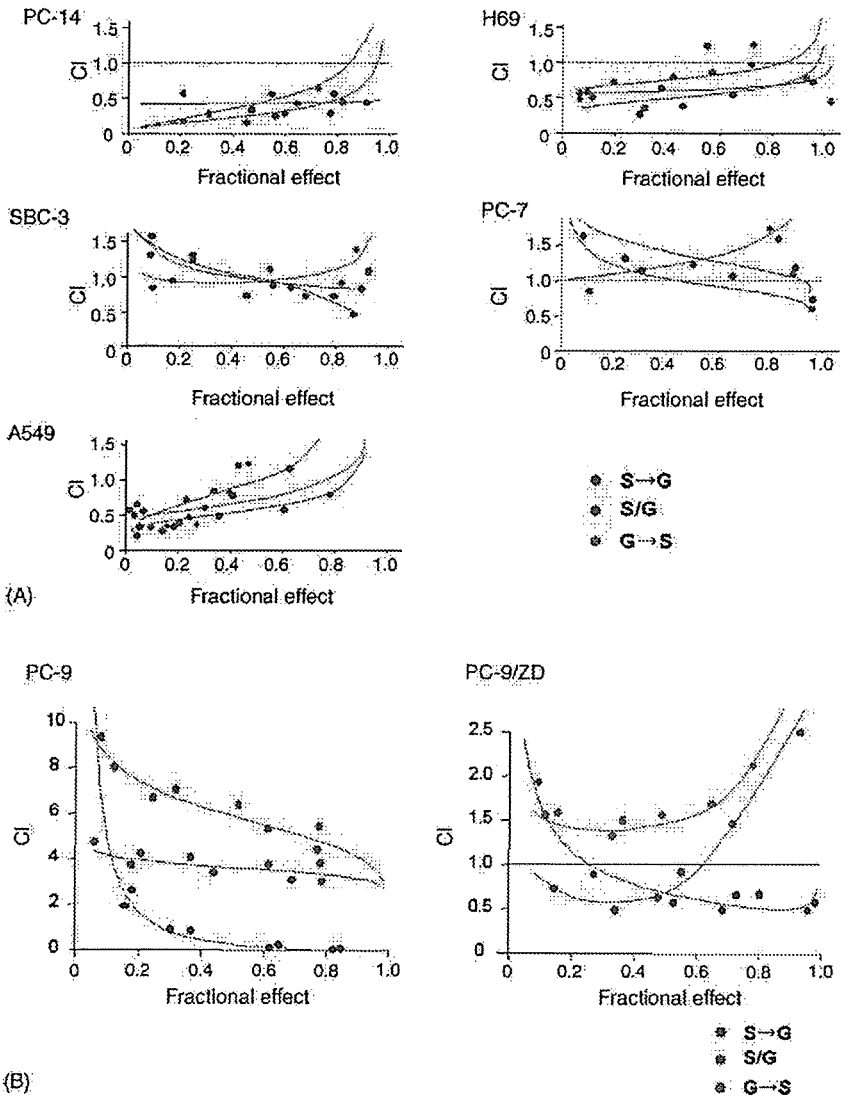

Fig. 1 Combination index (CI) plots of interactions between gefitinib and SN-38 in lung cancer cell lines. Each cell line was treated with gefitinib and SN-38, either alone or in combination at a fixed molar ratio. (A) (PC-14) gefitinib: SN-38 = 425:1; (SBC-3) 20000:1; (A549) 100:1; (H69) 2000:1; (PC-7) 3500:1. (B) (PC-9) gefitinib: SN-38 = 6:1; (PC-9ZD) 175:1. Treatment schedule: (1) SN-38 was applied first and gefitinib was applied 12 h later, followed by incubation in medium for 72 h (blue). (2) SN-8 and gefitinib were applied concurrently, followed by incubation in medium for 72 h (red). (3) Gefitinib was applied first and SN-38 was applied 12 h later, followed by incubation in medium for 72 h (green). S → G: sequential combination (SN-38 followed by gefitinib); C/G: concurrent combination; G → S: sequential combination (gefitinib followed by SN-38).

cells were stained with anti-Ki-67, anti-CD31 and the TUNEL assay (Fig. 3A and B). A reduction in tumor cell proliferation (Ki-67 staining), a reduction in tumor vasculature (CD31 staining), and an increase in tumor apoptosis (TUNEL staining) were observed in tumors treated with gefitinib alone or gefitinib and CPT-11. The administration of CPT-11 alone increased the number of Ki-67 positive tumor cells. In the PC-9 tumors, sequential treatment resulted in a 2.7-fold increase in tumor cell apoptosis and a 1.9-fold decrease in vessel staining, compared with the results obtained in tumors treated concurrently. The ratio of apoptosis:proliferation increased 1.7-fold in sequentially treated tumors compared with tumors treated with both drugs concurrently. Quantitative analysis of tumor cell proliferation and apoptosis showed a significant difference between the effects of the concurrent and sequential schedules ($P < 0.001$), but not between concurrent and gefitinib-alone ($P > 0.01$ for all comparisons, Fig. 3C). No significant difference in CD31-positive cells was observed between the control and gefitinib-alone treatments, suggesting that gefitinib exerts no remarkable anti-angiogenetic effects ($P > 0.01$, Fig. 3C). Similar findings were observed in PC-9/ZD tumors. These findings suggest that the antitumor activity of sequential treatment using gefitinib and CPT-11 is mediated by an increase in tumor cell apoptosis, compared with concurrent treatment.

4. Discussion

The EGFR-targeting drug gefitinib has been approved in many countries for the treatment of NSCLC patients who have previously received chemotherapy. Previous preclinical models have demonstrated the synergistic effects of gefitinib and platinums or taxanes [8,9]. However, no significant difference in survival was demonstrated in two randomized placebo-controlled phase II trials examining over 2000 previously untreated patients with NSCLC. In these trials, gefitinib was given in combination with paclitaxel and carboplatin or with gemcitabine and cisplatin [10,11]. Different administration schedules for gefitinib and cytotoxic agents may be necessary for select populations.

EGFR gene mutations have been demonstrated in NSCLC, and patients with lung cancers expressing mutant EGFR are strongly suspected to be hypersensitive to gefitinib alone. An in-frame short deletion in exon 19 of EGFR is strongly related to hyperresponsiveness to gefitinib and other tyrosine kinase inhibitors [12,13]. Cells expressing this deletional EGFR mutation are hypersenstivie to EGFR-targeted tyrosine kinase inhibitors [5]. On the other hand, the treat-

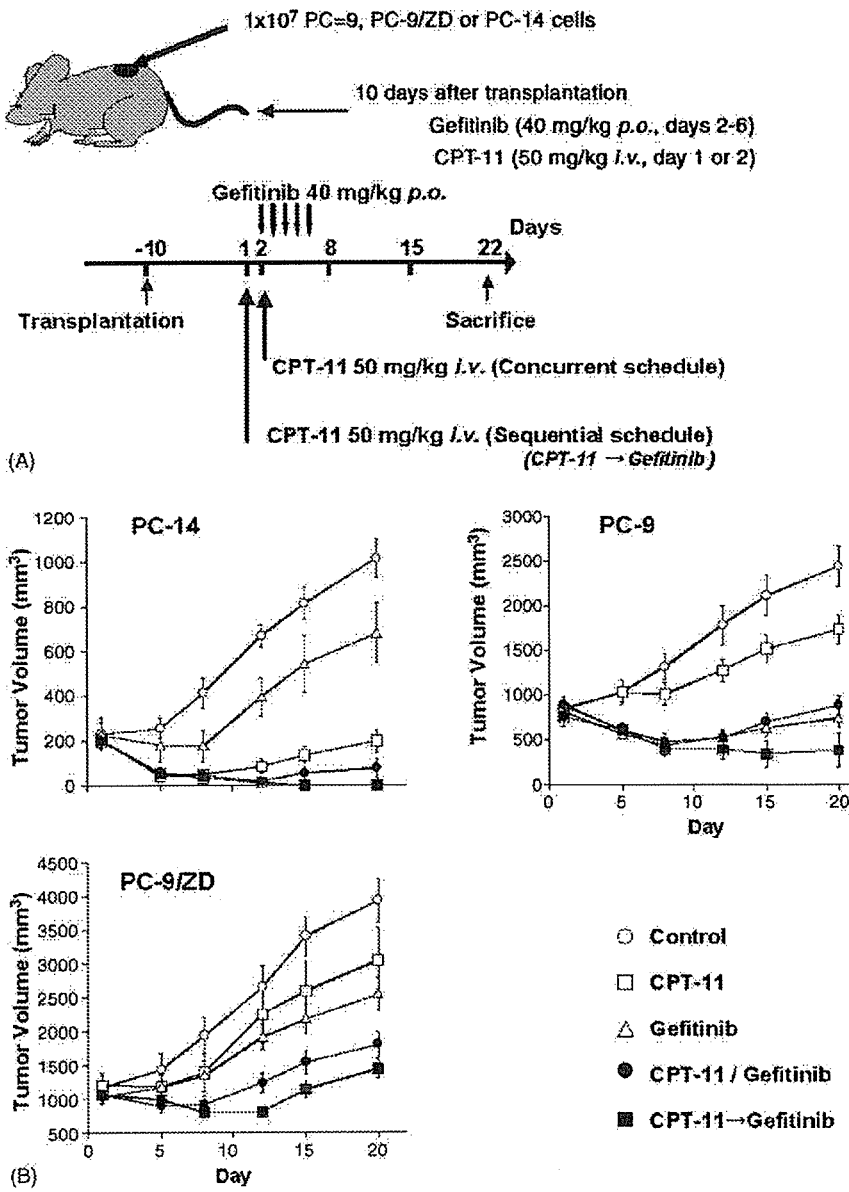

Fig. 2 Dose-dependent effects of combination therapy in PC9 and PC9/ZD cells in vivo. (A) Treatment schedule; (B) significant tumor growth-inhibition was observed in mice treated with the combination of gefitinib and CPT-11. Mice were allocated to five groups (6 mice/group) (○: 5% (w/v) glucose solution; □: CPT-11 50 mg/kg; △: gefitinib 40 mg/kg; ■: ZD1839 40 mg/kg + CPT-11 50 mg/kg concurrently; ●: CPT-11 50 mg/kg followed by ZD1839 40 mg/kg). (C) Treatment-related body weight loss in mice treated with gefitinib and/or SN-38. (○: 5% (w/v) glucose solution; □: CPT-11 50 mg/kg; △: ZD1839 40 mg/kg; ■: ZD1839 40 mg/kg + CPT-11 50 mg/kg concurrently; ●: CPT-11 50 mg/kg followed by ZD1839 40 mg/kg). Bars: ±S.D.